NATIONAL ADVISORY COMMITTEE FOR AERONAUTICS

TECHNICAL NOTE

No. 1817

PLASTIC BUCKLING OF SIMPLY SUPPORTED COMPRESSED PLATES

By Richard A. Pride and George J. Heimerl

Langley Aeronautical Laboratory
Langley Air Force Base, Va.

Washington
April 1949

NATIONAL ADVISORY COMMITTEE FOR AERONAUTICS

TECHNICAL NOTE NO. 1817

PLASTIC BUCKLING OF SIMPLY SUPPORTED COMPRESSED PLATES

By Richard A. Pride and George J. Heimerl

SUMMARY

An investigation was made to ascertain the validity of various theories for the plastic buckling of compressed simply supported plates by means of local-instability tests of drawn square tubes of 14S-T6 aluminum alloy.

The results obtained were in excellent agreement with Stowell's unified theory for the plastic buckling of columns and plates (NACA TN No. 1556). This agreement, in addition to that previously obtained for columns and flanges, is considered a satisfactory experimental verification of this theory which is based on a deformation theory of plasticity. Two other plastic buckling theories of the deformation type and the empirical secant-modulus method also gave a close correlation with the test results, but a plastic buckling theory of the flow type showed a lack of agreement.

INTRODUCTION

A theory was recently presented in reference 1 for the plastic buckling under compression of plates with different conditions of support and restraint along the unloaded edges. Good experimental verification of the theory was available at that time for the special cases of plates with the two unloaded edges free (columns) and of plates with one unloaded edge free and the other simply supported (flanges). No suitable experimental data were then available, however, for plates with both unloaded edges supported.

Various methods have been used to make buckling tests of simply supported plates in compression. One method utilizes plate-edge support fixtures. (See, for example, reference 2.) Such fixtures have not always proved satisfactory because of restraints and supporting conditions developed along the unloaded edges. A method which overcomes this difficulty and has proved quite satisfactory for the determination of buckling makes use of seamless square tubes, for which each of the four plates may be considered simply supported. (See p. 333, reference 3.)

In order to obtain experimental data in the plastic range for the case of the compressed simply supported plate to provide additional evidence as to the validity of the theory of reference 1, tests were made

of drawn square tubes of 14S-T6 aluminum alloy. The present paper gives the results of these tests and shows the correlation found with various available theories for plastic buckling.

SYMBOLS

b	width of plate, taken as average inside dimension for square tubes (fig. 1); use of inside dimensions is consistent with previous method for dimensioning extrusions (reference 4) and gives best agreement with test results in elastic range
L	length of plate
t	thickness of plate
k	plate buckling coefficient depending on plate edge conditions and plate proportions, taken as 4 for long simply supported plates (p. 333, reference 3)
η	nondimensional coefficient; number by which critical stress computed for elastic case must be multiplied to give critical stress for plastic case (for stresses in elastic range, $\eta = 1$, whereas above elastic range, $\eta < 1$)
μ	Poisson's ratio (taken as 0.33)
E	Young's modulus of elasticity taken in compression as 10,700 ksi for 14S-T6 aluminum alloy
E_s	secant modulus, slope of line connecting origin with any point on stress-strain curve
E_t	tangent modulus, slope of stress-strain curve at any point
σ_{cy}	compressive yield stress (0.2 percent offset)
σ_{cr}	critical compressive stress
$\bar{\sigma}_{max}$	average compressive stress at maximum load
ϵ_{cr}	calculated elastic critical compressive strain

TESTS

Specimens.- The specimens were cut from five different cross-sectional sizes of drawn square tube of 14S-T6 aluminum alloy (formerly designated 14S-T) supplied in random lengths of from 12 to 20 feet, and all having a nominal thickness of 0.156 inch. The cross section and method of dimensioning are illustrated in figure 1; dimensions of the local-instability specimens are given in table I together with data on the compressive yield stress for the various tubes (A, B, C, and so on) from which the specimens were taken. All specimens were tested with the ends ground flat and square in hydraulic testing machines having an accuracy within three-fourths of 1 percent.

Stress-strain tests.- Compressive stress-strain curves of the material were obtained both from compression tests of 8-inch tube specimens cut from each end of the tubes and from tests of individual, single-thickness specimens 2.52 inches long by 0.80 inch wide cut from various positions around a tube cross section. Tests were made of the 8-inch specimens in order to obtain representative longitudinal stress-strain curves for the entire tube, which would take into account the variation of properties, such as were found around the cross section for extruded 14S-T aluminum alloy. (See fig. 3, reference 4.) In order to prevent buckling of the tube, it was necessary to apply lateral support to the plates (fig. 2). Autographic load-strain curves were obtained from four wire strain gages (one on each face) recorded individually. Tests were made of the single-thickness specimens for three purposes: to insure that the 8-inch tube specimens were giving representative longitudinal stress-strain curves, to study the variation of longitudinal properties around the cross section, and to study the isotropy of the material. For the single-thickness tests, two differential-transformer gages were used with a compression fixture and recorder to provide autographic curves.

Local-instability tests.- The plate compressive strengths were determined from local-instability tests of the square tube specimens. (See illustration, fig. 3.) The critical compressive stress was determined by the "top-of-the-knee" method discussed in reference 5 from autographic load-displacement curves obtained for two adjacent plates of each tube. A sketch made from an actual record is presented in figure 4. Lateral displacements of the plates were measured by means of surface bearing bars held in direct contact with the plate surface by flexible cantilevers. (See fig. 3.) The resulting change in strain at the root of the cantilevers was recorded. The average stress at maximum load was obtained from the maximum load recorded by the testing machine.

The minimum length-to-width ratio L/b to insure tests of essentially long, simply supported plates and avoid the increase in strength due to short plate length was established as 4 in figure 5, which presents data obtained for various lengths of tube C.

In the measurements for the square tubes, the widths were found to vary less than ±0.5 percent but the thickness varied as much as 7 percent from the center of a face to the corners. This thickness variation was taken into account by calculating a mean thickness based on the cross-sectional area of the specimens and the measured widths. A small transverse (cylindrical) curvature was found in some of the tube walls; the theoretical increase in the critical compressive stress resulting from the maximum observed curvature was less than 1 percent and was therefore neglected. The characteristics of the tubes at buckling, as evidenced by the load-displacement curves, were very close to those expected from theoretically perfect specimens (fig. 4).

ANALYSIS

Stress-strain properties.- A knowledge of the basic compressive properties of a material is needed in order to correlate local-instability tests with theory.

Compressive stress-strain curves obtained from tests of the 8-inch-long cross sections are shown for the various tubes in figure 6. In order to illustrate the amount of variation of material properties, upper- and lower-limit stress-strain curves obtained from tests of single-thickness specimens cut from tube C are compared with the representative stress-strain curve for the entire cross section of tube C. (See fig. 6.) A survey of the compressive yield stress σ_{cy} around the tube cross section (fig. 7) obtained from tests of the single-thickness specimens indicated unusually uniform properties for this material. Tests of specimens cut transversely from the sides of the same tube showed an average increase of only 0.7 ksi in the compressive yield stress; thus, the material was indicated to be nearly isotropic. (See fig. 7.) The variation of σ_{cy} between the ends of any one tube was less than 1 ksi and between different tubes was only 3.2 ksi.

In a generalized correlation of the test results with the various plastic-buckling theories, the representative stress-strain curve of tube C (fig. 6) was used to determine values of the secant modulus and the tangent modulus shown in ratio form in figure 8.

Local-instability tests.- In the method of analysis used herein, the experimental critical compressive stress σ_{cr} is plotted against the calculated elastic critical compressive strain ϵ_{cr} for correlation with the compressive stress-strain curve for the material and the different theories of plastic buckling.

In order to calculate this elastic value of ϵ_{cr} which is dependent only on the geometry of the section, both sides of the plate buckling equation

$$\sigma_{cr} = \frac{k\pi^2\eta E t^2}{12(1 - \mu^2)b^2} \tag{1}$$

are divided by E, and η is taken equal to 1 to give

$$\epsilon_{cr} = \frac{k\pi^2 t^2}{12(1 - \mu^2)b^2} \tag{2}$$

EVALUATION OF η

In calculating the plastic buckling stresses for plates, it is convenient to use the plate buckling equation (see equation (1)) and evaluate the nondimensional coefficient η which is a measure of the reduced modulus ηE effective at buckling. For stresses in the elastic range $\eta = 1$, whereas above the elastic range $\eta < 1$. Values of η determined by the various theories (references 1 and 6 to 9) and by the secant-modulus method (reference 10) are given in the following sections for long, compressed, simply supported plates, and are shown graphically in figure 8.

Stowell theory.- On the assumption that in plates as well as in columns unloading does not occur in the early stages of buckling, Stowell (reference 1) obtained a solution for the plastic buckling of plates and columns which was based upon deformation stress-strain relations derived by Ilyushin. The theory is applicable to plates having various edge support and restraint conditions; reference 1 gives expressions for η for a number of different cases. For a long, simply-supported plate,

$$\eta = \frac{E_s}{E}\left(\frac{1}{2} + \frac{1}{2}\sqrt{\frac{1}{4} + \frac{3}{4}\frac{E_t}{E_s}}\right) \tag{3}$$

where

E Young's modulus

E_s secant modulus

E_t tangent modulus

Ilyushin theory.- Ilyushin (reference 6) has developed a theory for plastic buckling of plates and shells based upon deformation stress-strain relations which differs from Stowell's theory principally in the concept that unloading on one side of the plate does occur at the beginning of buckling. An expression for η, derived from Ilyushin's results (reference 6), may be expressed as

$$\eta = \frac{1 - X}{2}\left(1 + \sqrt{\frac{1 - X + 3j}{4(1 - X)}}\right) \tag{4}$$

where

$$X = \left(1 - \frac{E_s}{E}\right)\left(1 - \frac{\sqrt{j}}{2}\right)\left[\left(1 - \frac{\sqrt{j}}{2}\right)^2 + \frac{3}{4}\frac{j}{1 - \left(1 - \frac{\sqrt{j}}{2}\right)\left(1 - \frac{E_s}{E}\right)}\right]$$

$$j = \frac{4\frac{E_t}{E}}{\left(1 + \sqrt{\frac{E_t}{E}}\right)^2}$$

Bijlaard theory.- Bijlaard presented a deformation-type theory of plastic buckling in 1938 (references 7 and 8) which has only recently received attention in this country. This theory gives results from which η may be written as

$$\eta = \frac{1}{2}\left(1 - \mu^2\right)\left(\sqrt{AD} + B + 2F\right) \tag{5}$$

where

μ Poisson's ratio (elastic value)

$$A = \frac{1 + g(4 + 3e)}{5 - 4\mu + 3e + g\left[4(1 - \mu^2) + 3e\right]}$$

$$B = \frac{2(1 + 2\mu g)}{5 - 4\mu + 3e + g\left[4(1 - \mu^2) + 3e\right]}$$

$$D = \frac{4(1 + g)}{5 - 4\mu + 3e + g\left[4(1 - \mu^2) + 3e\right]}$$

$$F = \frac{1}{2 + 2\mu + 3e}$$

$$e = \frac{E}{E_s} - 1$$

$$g = \frac{\frac{E_t}{E}}{1 - \frac{E_t}{E}}$$

Handelman-Prager theory.- Handelman and Prager have developed a theory for plastic buckling (reference 9) based upon flow-type stress-strain relations. For this theory, η may be given as

$$\eta = \frac{1}{4}\left(D'_{11} + 2D'_{12} + D'_{22}\right) \tag{6}$$

where

$$D'_{11} = 1 - c\delta(2 - \mu)^2$$

$$D'_{12} = 1 - c\delta(2 - \mu)(2\mu - 1)$$

$$D'_{22} = 1 - c\delta(2\mu - 1)^2$$

$$\delta = \frac{1}{2}\left[1 - \frac{3}{2}\left(\alpha + \sqrt{\alpha^2 - 1}\right) + \frac{1}{2}\left(\alpha + \sqrt{\alpha^2 - 1}\right)^3\right]$$

$$\alpha = 1 - \frac{2}{c(5 - 4\mu)}$$

$$c = \frac{\frac{E}{E_t} - 1}{\frac{E}{E_t}(5 - 4\mu) - (1 - 2\mu)^2}$$

Secant-modulus method.- An empirical method for determining plastic buckling stresses of plates was suggested by Gerard (reference 10) and has been found to work quite well for plate assemblies of H-, Z-, and C-sections for a number of aircraft structural materials. (See reference 4.) This method defines η as

$$\eta = \frac{E_s}{E} \tag{7}$$

RESULTS

The results of the local-instability tests are summarized for the critical compressive stress in table I and figure 6 and for the average stress at maximum load in table I. The correlation of the results with the theories for plastic buckling and the secant-modulus method is shown in figure 9.

For direct comparison with the applicable stress-strain curves for the material, the experimental critical compressive stress σ_{cr} is plotted against the calculated elastic critical compressive strain ϵ_{cr} (see equation (2)) in figure 6 where the test points are seen to fall somewhat below the stress-strain curves in the plastic region.

The generalized correlation with the single representative compressive stress-strain curve, the theories for plastic buckling, and the secant-modulus method is made in figure 9 by adjusting the test results to allow for variations in the compressive yield stress of the material for the various tubes by the method described in reference 11. In this generalized comparison the test results in the plastic region can be seen to fall a little below the stress-strain curve which also gives the results of the secant-modulus method; the test results lie closest to the calculated plate buckling curve σ_{cr} against ϵ_{cr} given by Stowell's theory. Ilyushin's and Bijlaard's theories give results which are slightly higher but still fall below the compressive stress-strain curve. Thus, good agreement with the test results is shown for the three deformation-type theories of plastic buckling. There is little correlation, however, between the test results and the Handelman-Prager theory, and the difference between this flow-type theory and deformation-type theories is marked. (See fig. 9.)

With regard to the accuracy of the test results for σ_{cr}, the nearly ideal load-displacement curves obtained for many of the tests (fig. 4) and the unusual degree of isotropy of the material (fig. 7) lead to the belief that the test specimens came close to being theoretically ideal specimens, and therefore the test results provide a good basis for discriminating between the various theories on plastic buckling of plates.

CONCLUSIONS

The results of the local-instability tests of drawn square tubes warrant the following conclusions as regards the plastic buckling of a long, flat, simply supported compressed plate:

1. The results of these tests show good agreement with Stowell's theory for the plastic buckling of a simply supported plate which is based on a deformation theory of plasticity. This confirmation, together with that previously shown for a flange and column, is considered to constitute a satisfactory experimental verification of the theory.

2. Good agreement with the test results is evidenced in general by the deformation-type theories for plastic buckling. Stowell's theory is in the closest agreement with the test results reported herein, but Ilyushin's and Bijlaard's theories give results only slightly higher.

3. Marked disagreement is shown between the test results and the Handelman-Prager theory which is based on a flow theory of plasticity.

4. Buckling stresses calculated by the empirical secant-modulus method are reasonable, though higher than the test results. This convenient rapid method can therefore be used for an approximate determination of the critical compressive stress.

Langley Aeronautical Laboratory
Nation Advisory Committee for Aeronautics
Langley Air Force Base, Va., January 18, 1949

REFERENCES

1. Stowell, Elbridge Z.: A Unified Theory of Plastic Buckling of Columns and Plates. NACA TN No. 1556, 1948.

2. Kollbrunner, C. F.: Das Ausbeulen der auf einseitigen, gleichmässig verteilten Druck beanspruchten Platten im elastischen und plastischen Bereich. Mitt. Nr. 17, Inst. für Baustatik an der E.T.H., Gebr. Leemann & Co. (Zürich), 1946.

3. Timoshenko, S.: Theory of Elastic Stability. McGraw-Hill Book Co., Inc., 1936.

4. Heimerl, George J.: Determination of Plate Compressive Strengths. NACA TN No. 1480, 1947.

5. Hu, Pai C., Lundquist, Eugene E., and Batdorf, S. B.: Effect of Small Deviations from Flatness on Effective Width and Buckling of Plates in Compression. NACA TN No. 1124, 1946.

6. Ilyushin, A. A.: The Theory of Elasto-Plastic Strains and Its Application. Bulletin of the Academy of Sciences, USSR, Section of Technical Sciences, June 1948, pp. 769-788.

7. Bijlaard, P. P.: A Theory of Plastic Buckling with Its Application to Geophysics. Koninklijke Nederlandsche Akad. Wetenschappen. Reprinted from Proc., vol. XLI, no. 5, 1938, pp. 468-480.

8. Bijlaard, P. P.: A Theory of Plastic Stability and Its Application to Thin Plates of Structural Steel. Koninklijke Nederlandsche Akad. Wetenschappen. Reprinted from Proc., vol. XLI, no. 7, 1938, pp. 731-743.

9. Handelman, G. H., and Prager, W.: Plastic Buckling of a Rectangular Plate under Edge Thrusts. NACA TN No. 1530, 1948.

10. Gerard, George: Secant Modulus Method for Determining Plate Instability above the Proportional Limit. Jour. Aero. Sci., vol. 13, no. 1, Jan. 1946, pp. 38-44 and 48.

11. Heimerl, George J.: Methods of Constructing Charts for Adjusting Test Results for the Compressive Strength of Plates for Differences in Material Properties. NACA TN No. 1564, 1948.

TABLE I.- DIMENSIONS AND LOCAL-INSTABILITY TEST RESULTS

FOR 14S-T6 ALUMINUM-ALLOY SQUARE TUBE SPECIMENS

Specimen	Tube	L (in.)	b (in.) (a)	t (in.) (b)	L/b	b/t	ϵ_{cr} (c)	σ_{cr} (ksi)	Adjusted σ_{cr} (ksi) (d)	$\bar{\sigma}_{max}$ (ksi)	σ_{cy} (ksi) (fig. 6)
1a	A	26.84	6.69	0.1575	4.0	42.5	0.00205	21.2	21.2	31.6	62.2
1b	A	26.84	6.69	.1573	4.0	42.5	.00205	22.0	22.0	31.5	62.2
2a	B	30.06	6.69	.1600	4.5	41.8	.00211	22.6	22.6	31.7	60.7
2b	B	30.05	6.69	.1600	4.5	41.8	.00211	22.5	22.5	31.6	60.7
3a	C	4.74	4.68	.1557	1.0	30.1	.00406	54.6	54.6	54.6	61.4
4a	C	9.41	4.68	.1557	2.0	30.1	.00406	48.1	48.1	48.3	61.4
4b	C	9.35	4.68	.1555	2.0	30.1	.00406	48.2	48.2	48.4	61.4
5a	C	14.10	4.68	.1553	3.0	30.1	.00406	44.6	44.6	45.2	61.4
5b	C	14.11	4.68	.1553	3.0	30.1	.00406	45.1	45.1	45.5	61.4
6a	C	18.96	4.68	.1555	4.0	30.1	.00406	42.8	42.8	43.8	61.4
6b	C	18.94	4.68	.1557	4.0	30.1	.00406	42.9	42.9	43.5	61.4
7a	C	23.45	4.68	.1553	5.0	30.1	.00406	42.4	42.4	43.5	61.4
7b	C	23.44	4.68	.1559	5.0	30.1	.00406	42.8	42.8	43.2	61.4
8a	D	17.83	3.94	.1539	4.5	25.6	.00563	53.3	52.2	53.9	63.2
8b	D	17.83	3.94	.1539	4.5	25.6	.00563	53.9	52.8	54.7	63.2
9a	E	15.50	3.44	.1526	4.5	22.5	.00729	57.0	58.1	57.6	60.0
9b	E	15.50	3.44	.1528	4.5	22.5	.00729	57.8	59.0	57.9	60.0
10a	F	14.42	3.19	.1531	4.5	20.8	.00853	61.4	59.9	61.6	63.0
10b	F	14.42	3.19	.1530	4.5	20.8	.00853	60.8	59.3	61.0	63.0
11a	F	19.16	3.19	.1534	6.0	20.8	.00853	60.8	59.3	60.9	63.0

[a] Width is measured inside face to inside face of tubes (fig. 1).

[b] Thickness is the mean thickness calculated from the cross-sectional area.

[c] $\epsilon_{cr} = \dfrac{k\pi^2 t^2}{12(1-\mu^2)b^2}$

[d] Critical compressive stress adjusted for variations of compressive yield stress of material by methods of reference 11.

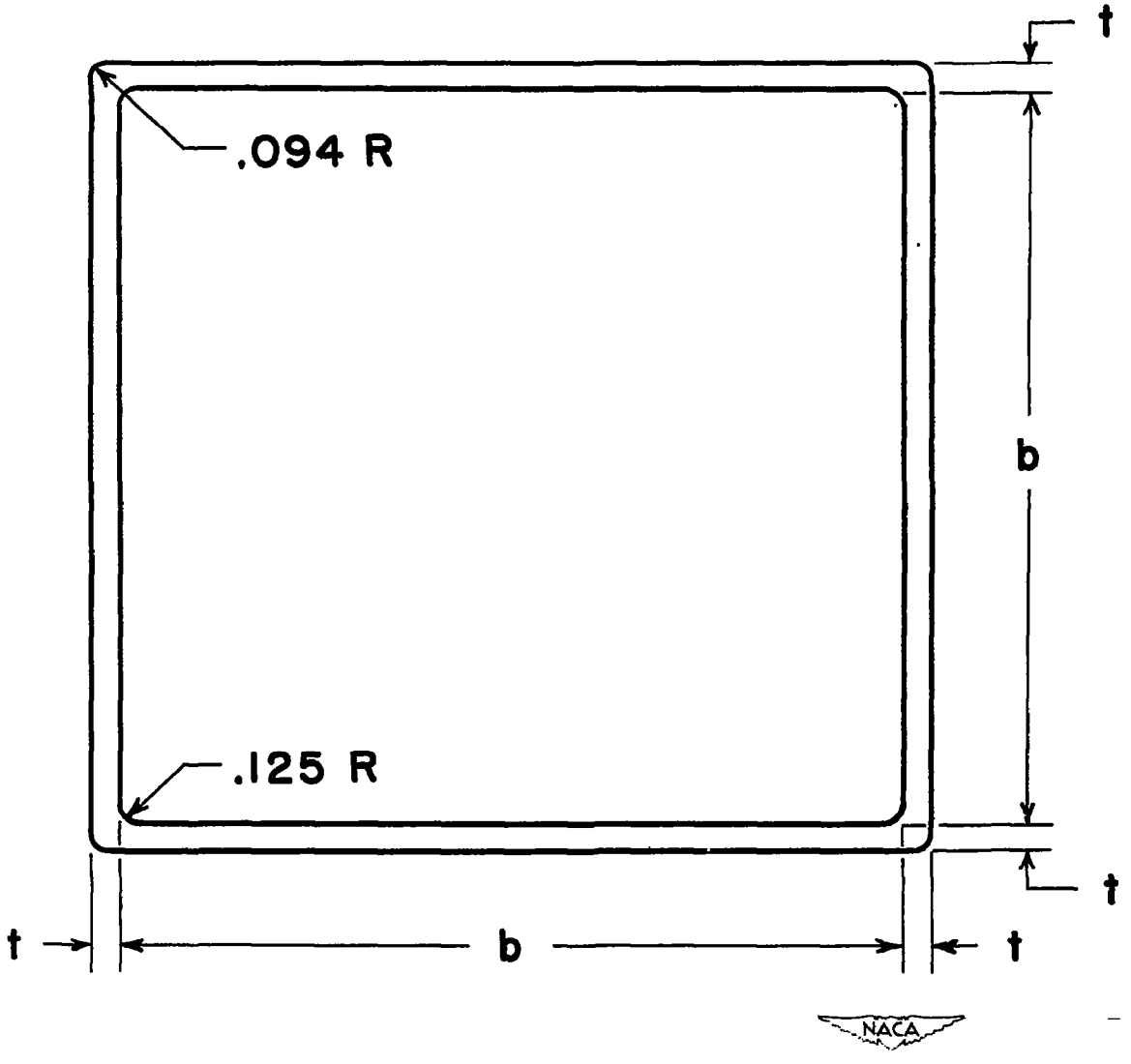

Figure 1.— Cross section of square tube.

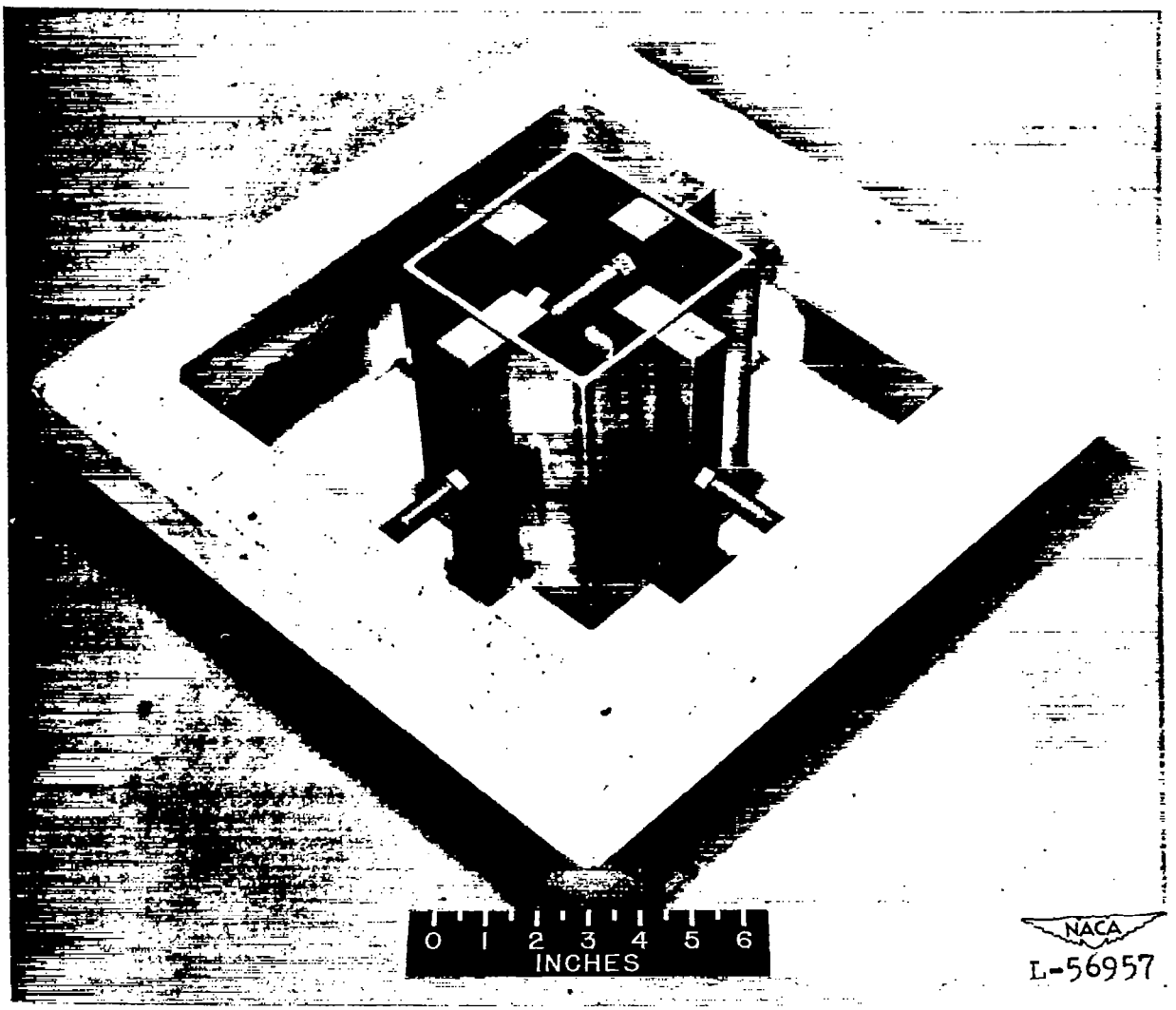

Figure 2.— Method of supporting individual plates of a square tube for compression stress—strain tests.

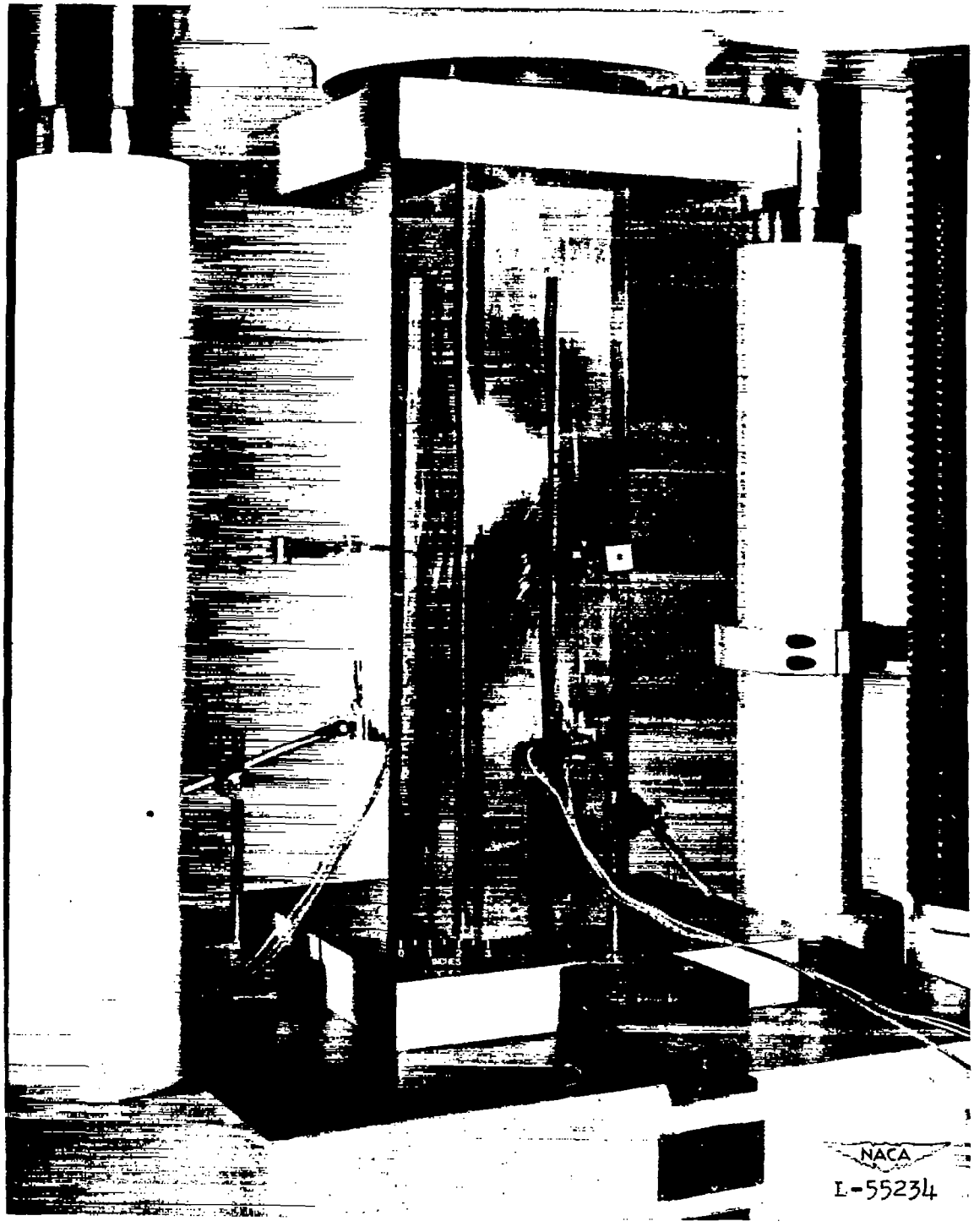

Figure 3.– Method of detecting buckling of plate elements of a square tube under test.

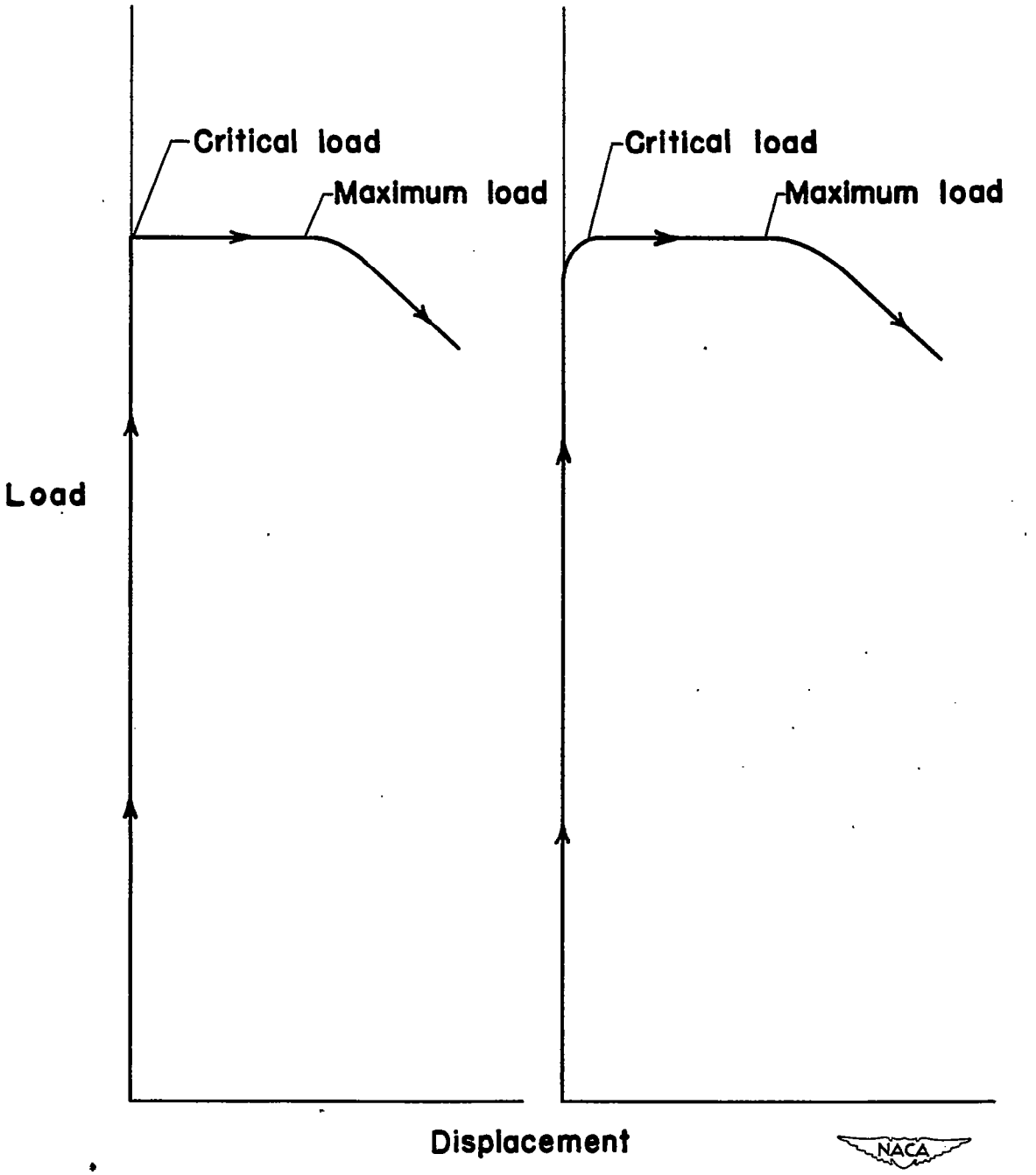

Figure 4.— Load-displacement curves for two adjoining plates of square tube specimen 9b.

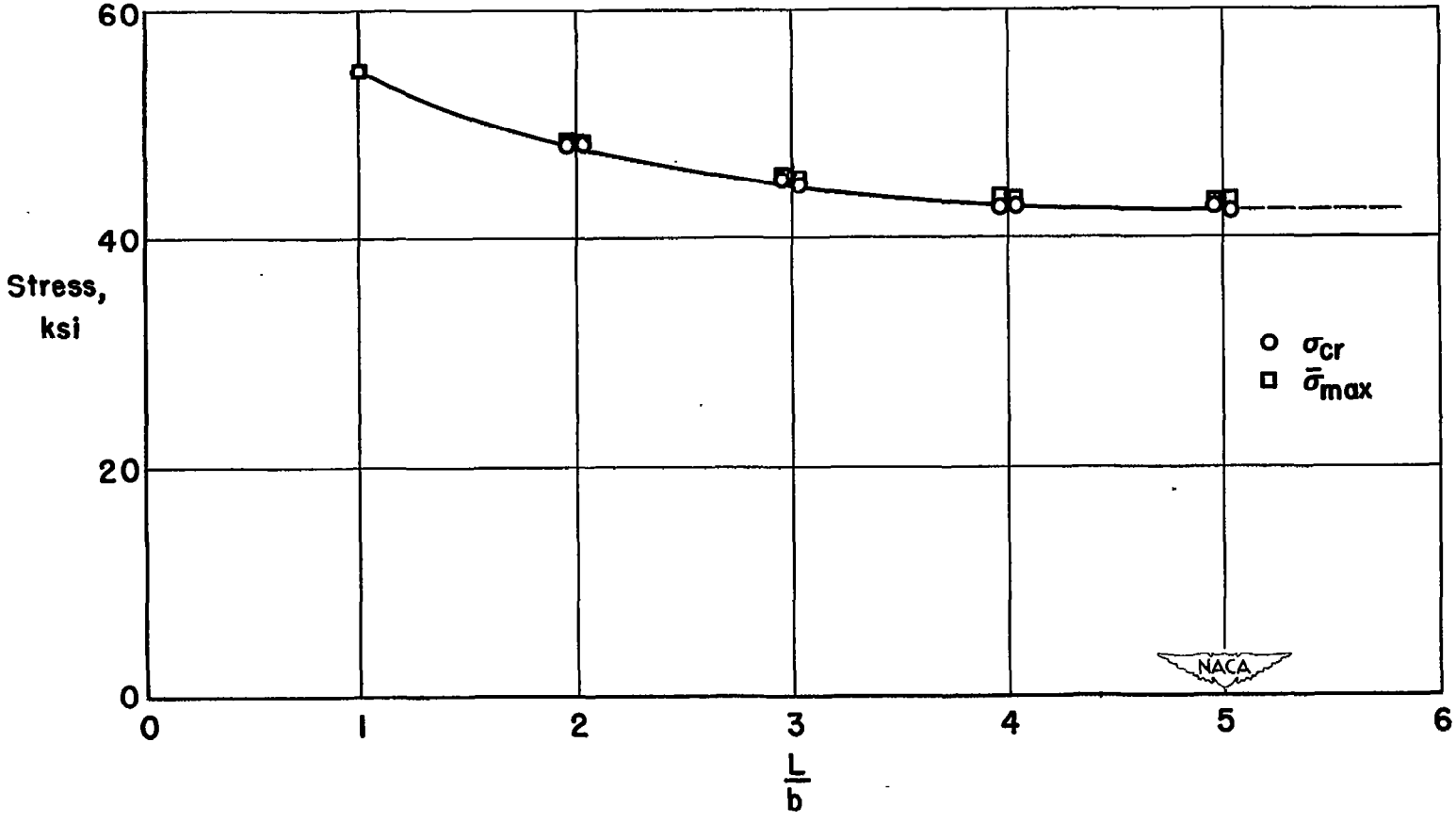

Figure 5.— Variation of critical compressive stress σ_{cr} and average stress at maximum load $\bar{\sigma}_{max}$ with the length-width ratio L/b for square tubes of 14S-T6 aluminum alloy (tube C).

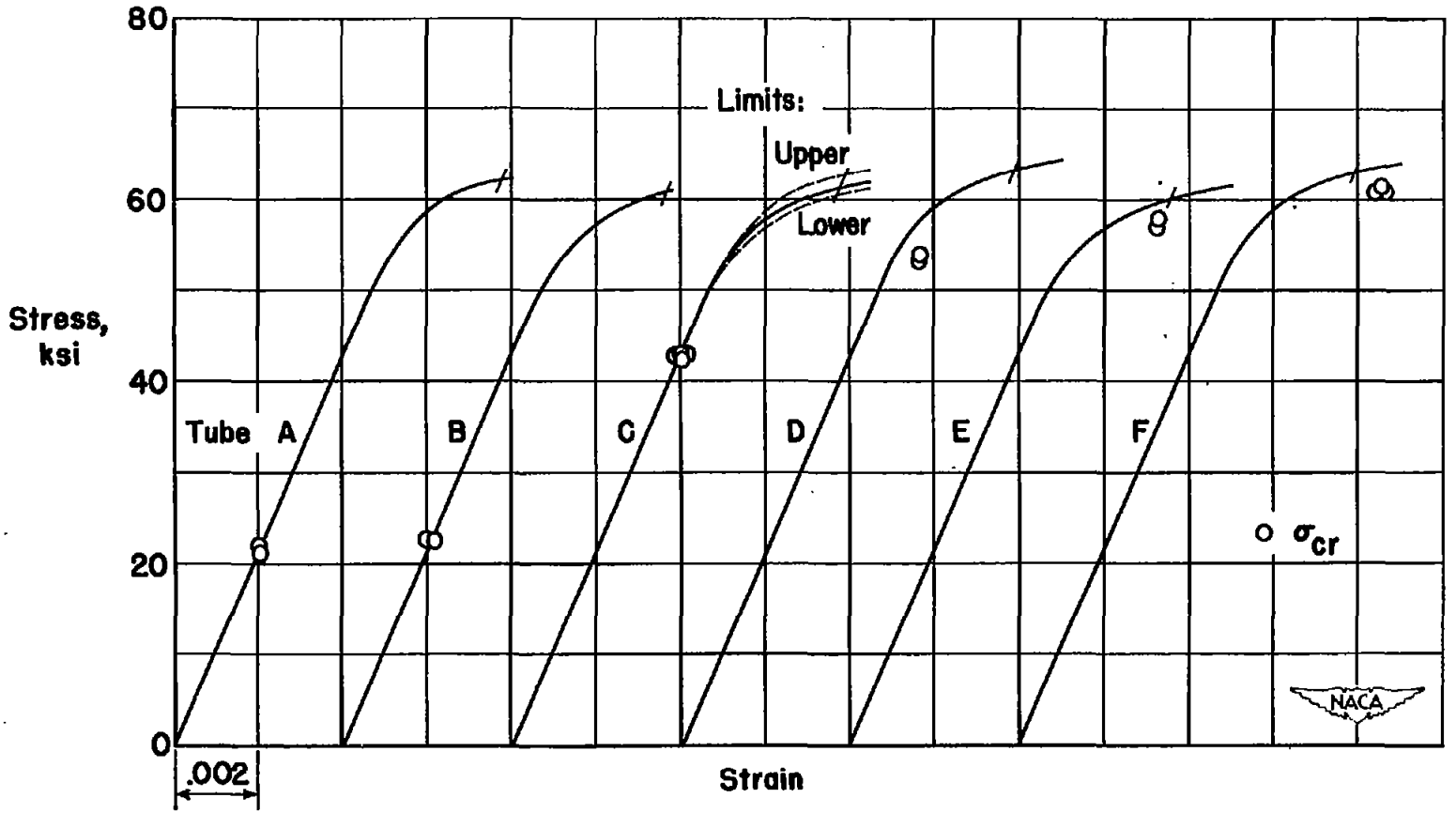

Figure 6.— Correlation of test results for the critical compressive stress for long, simply supported, flat plates with the compressive stress-strain curves for 14S-T6 aluminum alloy. (Calculated elastic critical compressive strain used for plate tests.)

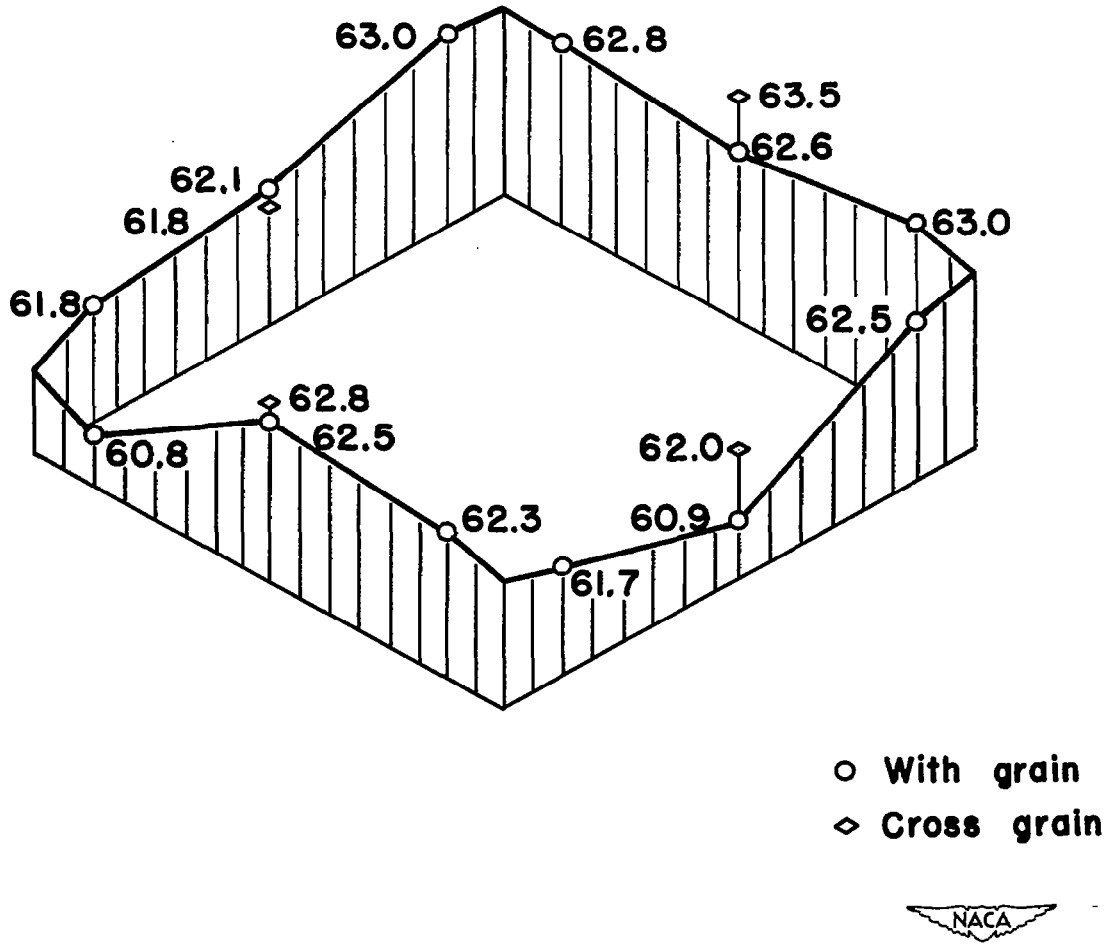

Figure 7.—Variation of the compressive yield stress in ksi over the cross section of a drawn 14S-T6 aluminum-alloy square tube (tube C).

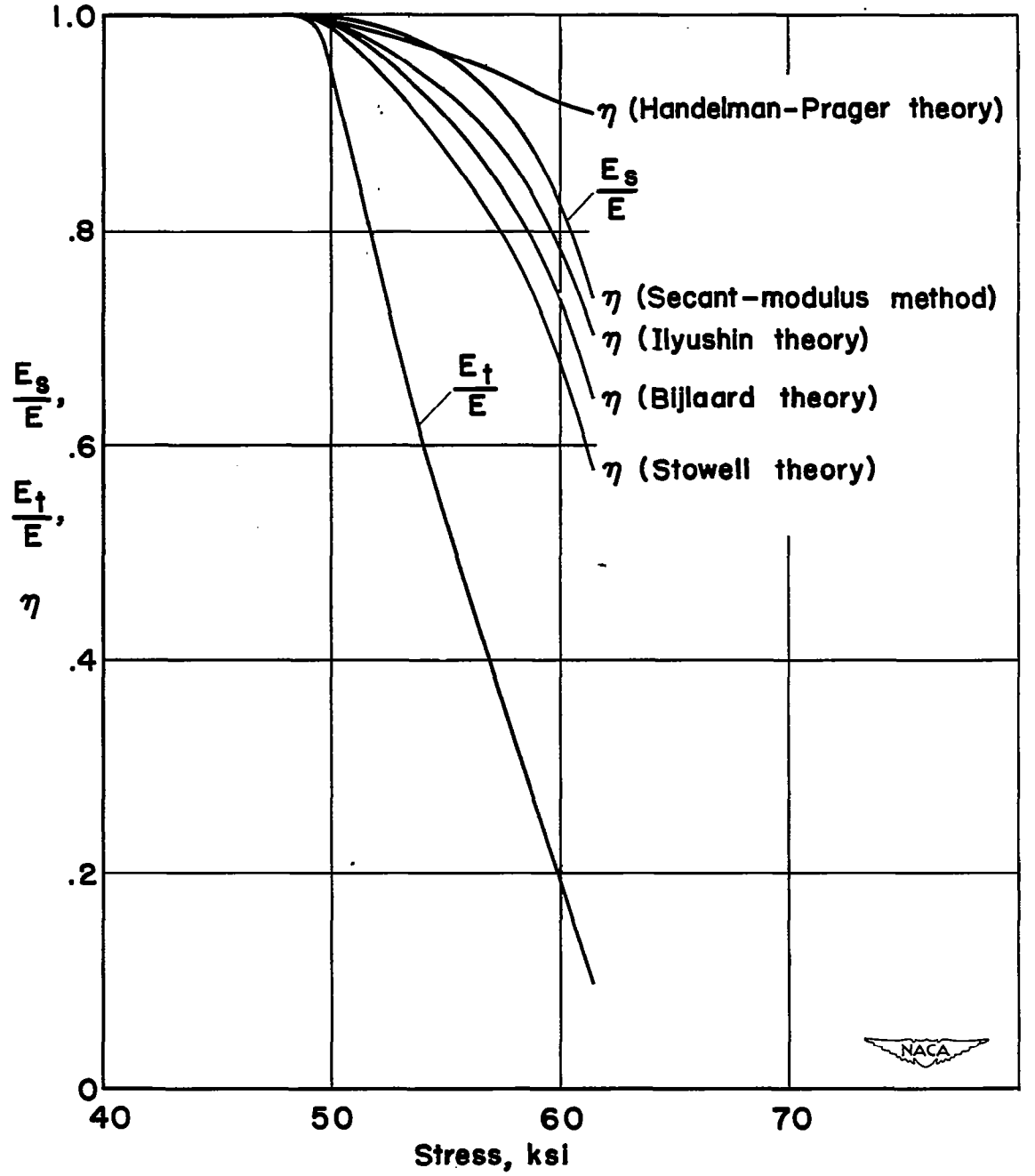

Figure 8.—Variation of $\frac{E_s}{E}$, $\frac{E_t}{E}$, and nondimensional coefficient η with stress for 14S-T6 aluminum alloy.

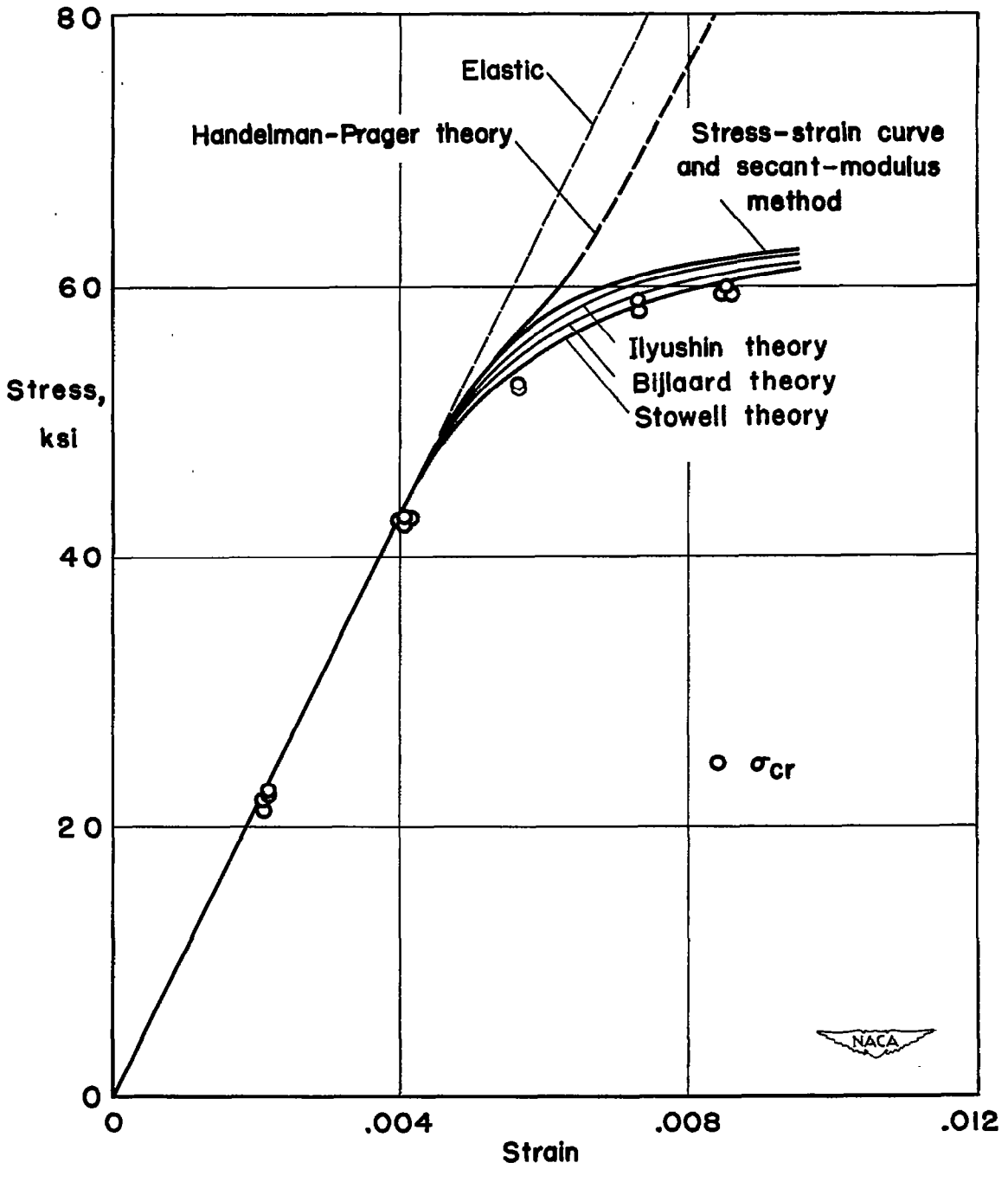

Figure 9.— Correlation of adjusted test results for the critical compressive stress with calculated plate buckling curves for long, simply supported, flat plates of 14S-T6 aluminum alloy. (Calculated elastic critical compressive strain used for plate tests.)